

directional compression at fixed diluent activity was also studied. Experimental results proved the equivalence of the response of the network to isotropic shrinking and to unidirectional compression.

An attempt was made to evaluate the relationship between elastic modulus, swelling pressure, and equilibrium concentration of the gel. The swelling pressure was expressed in terms of the elastic modulus of the gel equilibrated with pure swelling agent and the deformation ratio relative to the undeformed length of the freely swollen gel. The validity of the proposed relationships was confirmed by experimental results.

Acknowledgment. This work was supported by the Hungarian Academy of Sciences under Contracts AKA 1-3-86-229 and OTKA 1204/86.

Registry No. Toluene, 108-88-3; benzene, 71-43-2.

References and Notes

- (1) Flory, P. J.; Rehner, J. Jr. *J. Chem. Phys.* **1943**, *11*, 521.
- (2) Flory, P. J.; Rehner, J. Jr. *J. Chem. Phys.* **1944**, *12*, 412.
- (3) Gee, G. *Trans. Faraday Soc.* **1946**, *42B*, 33.
- (4) Treloar, L. R. G. *Trans. Faraday Soc.* **1950**, *50*, 783.
- (5) Treloar, L. R. G. *Proc. R. Soc. London, A* **1950**, *A200*, 176.
- (6) Rijke, A. M.; Taylor, G. L. *J. Polym. Sci., Polym. Chem. Ed.* **1967**, *5*, 1433.
- (7) Flory, P. J. *Principles of Polymer Chemistry*; Cornell University: Ithaca, NY, 1953.
- (8) Treloar, L. R. G. *The Physics of Rubber Elasticity*; Clarendon: Oxford, 1976.
- (9) de Gennes, P.-G. *Scaling Concepts in Polymer Physics*; Cornell University: Ithaca, NY, London, 1979.
- (10) de Gennes, P.-G. *Riv. Nuovo Cimento Soc. Ital. Fis.* **1977**, *7*, 363.
- (11) des Cloiseaux, J. *J. Phys. (Les Ulis, Fr.)* **1975**, *36*, 281.
- (12) Roots, J.; Nyström, B. *Polymer* **1979**, *20*, 148.
- (13) Candau, S.; Bastide, J.; Delsanti, M. *Adv. Polym. Sci.* **1982**, *44*, 27.
- (14) Dusek, K.; Prins, W. *Adv. Polym. Sci.* **1969**, *6*, 1.
- (15) Munch, J. P.; Candau, S.; Herz, J.; Hild, G. *J. Phys. (Les Ulis, Fr.)* **1977**, *38*, 971.
- (16) Hecht, A. M.; Geissler, E. *J. Phys. (Les Ulis, Fr.)* **1978**, *39*, 631.
- (17) Zrinyi, M.; Horkay, F. *Polym. Bull. (Berlin)* **1980**, *3*, 665.
- (18) Horkay, F.; Zrinyi, M. *Polym. Bull. (Berlin)* **1981**, *4*, 361.
- (19) Zrinyi, M.; Horkay, F. *J. Polym. Sci., Polym. Phys. Ed.* **1982**, *20*, 815.
- (20) Horkay, F.; Zrinyi, M. *Macromolecules* **1982**, *15*, 1306.
- (21) Zrinyi, M.; Horkay, F. *Macromolecules* **1984**, *17*, 2805.
- (22) Horkay, F.; Zrinyi, M. *J. Macromol. Sci., Phys.* **1986**, *B25(3)*, 307.
- (23) Horkay, F.; Nagy, M. *Polym. Bull. (Berlin)* **1980**, *3*, 457.
- (24) Horkay, F.; Nagy, M.; Zrinyi, M. *Acta Chim. Acad. Sci. Hung.* **1981**, *108*, 287.
- (25) Nagy, M.; Horkay, F. *Acta Chim. Acad. Sci. Hung.* **1980**, *104*, 49.
- (26) Vink, H. *Eur. Polym. J.* **1973**, *10*, 149.
- (27) Horkay, F.; Nagy, M. *Acta Chim. Acad. Sci. Hung.* **1980**, *103*, 387.
- (28) Zrinyi, M.; Horkay, F. *Polymer* **1987**, *28*, 1139.
- (29) Bastide, J.; Candau, S.; Leibler, L. *Macromolecules* **1981**, *14*, 719.
- (30) Bastide, J.; Duplessix, R.; Picot, C.; Candau, S. *Macromolecules* **1984**, *17*, 83.
- (31) Geissler, E.; Hecht, A. M. *Macromolecules* **1980**, *13*, 1276.
- (32) Geissler, E.; Hecht, A. M. *Macromolecules* **1981**, *14*, 185.

Diffusion of Homopolymers into Nonequilibrium Block Copolymer Structures. 1. Molecular Weight Dependence[†]

Peter F. Green*

Sandia National Laboratory, Albuquerque, New Mexico 87185

Thomas P. Russell

IBM Research Division, Almaden Research Center, 650 Harry Road, San Jose, California 95120-6099

Robert Jérôme and Maryse Granville

University of Liege, Liege, Belgium. Received November 20, 1987;
Revised Manuscript Received April 4, 1988

ABSTRACT: The diffusion of deuteriated polystyrene (d-PS) and deuteriated poly(methyl methacrylate) (d-PMMA) into nonequilibrium symmetric diblock copolymer structures was studied by using elastic recoil detection (ERD). The diffusion coefficient, D_{HC} , of the d-PS and d-PMMA homopolymer chains of degree of polymerization N_H diffusing into the copolymer hosts was found to vary as N_H^{-2} for chains where $N_H \leq N_C/2$. N_C is the total number of monomer segments of the copolymer chain. In cases where N_H was sufficiently larger than N_C the dependence of D_{HC} on N_H was considerably greater than N_H^{-2} . D_{HC} was found to be an order of magnitude lower than D_{HH} , the diffusion coefficient of the homopolymer chains diffusing into their respective homopolymer hosts. It was found that varying the rate of solvent evaporation, changing the solvent used for preparing the samples, and preannealing the samples for sufficiently long periods of time before the diffusion process had a marked influence on the diffusional transport properties.

Introduction

The diffusion of homopolymer chains into phase-separated copolymer structures has received virtually no attention. Studies done thus far have primarily been con-

cerned with the diffusion of homopolymer chains into homopolymer hosts.¹ It is clear from experiment that the tracer diffusion coefficient, D^* , of a chain of molecular weight M diffusing into a host of chains of sufficiently high molecular weight is described by $D^* = D_0 M^{-2}$. This is consistent with theory.^{2,3} D_0 is proportional to the molecular weight between entanglements and inversely proportional to the monomeric friction coefficient. Predictions

[†] The portion of the work performed at Sandia National Laboratories was supported by the United States Department of Energy under Contract DE-AC04-76DP00789.

of the magnitude of D_0 that require knowledge of viscoelastic parameters are in very good agreement with experiment.⁴

Placing physical constraints on the volume into which homopolymer chains diffuse is expected to have a marked influence on the diffusional transport properties of the homopolymer. Block copolymers that exhibit microphase separation are good systems to investigate such behavior. Depending on the relative molecular weights of the blocks in the copolymer the morphology can be either spherical, cylindrical, or lamellar. The molecular weight of the blocks will dictate the size of the phases present in these structures. In this paper, measurements of the diffusion of deuterated polystyrene (d-PS) and of deuterated poly(methyl methacrylate) (d-PMMA) into symmetric diblock copolymers of polystyrene and poly(methyl methacrylate) (PS/PMMA) were done by using elastic recoil detection (ERD). The effects of varying the molecular weights of the homopolymers and host copolymers were examined. In addition, the influence of the sample preparation conditions on the diffusional transport properties was investigated.

At equilibrium, symmetric diblock copolymers exhibit a microphase-separated morphology that is lamellar. The perfection of the lamellar ordering may be influenced by the preparation conditions of the films of the diblock. This in turn may affect the rate at which the homopolymer penetrates into the diblock host. The characterization of the bulk microphase separation was accomplished by using small-angle X-ray scattering (SAXS). Here, the sizes of the domains and the degree of perfection of the microphase separation, i.e., phase purity and the sharpness of the phase boundaries between the PS and PMMA phases, could be quantitatively assessed.

It is important to know the fraction of surface area through which the diffusant can freely diffuse. Since PS and PMMA have different surface energies, then the concentration of either species at the surface may be markedly different from that of the bulk. Transmission electron microscopy has been used previously on other copolymer systems to obtain such information.⁵ Unfortunately, due to sample degradation, measurements of this type are prohibitively difficult in the PS/PMMA case. X-ray photoelectron spectroscopy (XPS) was therefore used to determine the relative composition of each component at the air-copolymer interface.

Experimental Section

The PS/PMMA copolymers were prepared by sequential anionic polymerization of styrene and methyl methacrylate.⁶ After being dried on fluorenyllithium and distilled, the styrene was first polymerized at -78°C in a THF solution under the usual conditions of dryness and purged atmosphere; the initiator used was *sec*-butyllithium. The MMA, dried on triethylaluminum and distilled, was then added to form the block copolymer. Finally the reaction was stopped by adding HCl, and the copolymer was precipitated into methanol and dried. The molecular weight of the PS sequence was determined by GPC; the composition of the copolymers and the molecular weight of the PMMA were determined by NMR.

In this study, the molecular weights of the copolymers used were 42 000/42 000; 157 000/162 000, and 275 000/260 000 and are denoted as SMI, SMII, and SMIII, respectively. Here, the first number is the molecular weight of the PS block and the second that of the PMMA block. If N_{PS} and N_{PMMA} are the number of chain (monomer) segments that are PS or PMMA segments, respectively, then the fraction of chain segments in the block copolymer that are PS units is $f_{\text{PS}} = N_{\text{PS}}/(N_{\text{PS}} + N_{\text{PMMA}})$. f_{PS} for SMI, SMII, and SMIII are 0.49, 0.49, and 0.50, respectively. The polydispersity, M_w/M_n , for each of the block copolymers was ca. 1.2 in all cases. The d-PS used in this study were purchased

from Polymer Laboratories and used without further purification. The d-PMMA was prepared as discussed previously.⁷ The M_w/M_n for the d-PS and d-PMMA was better than 1.05 in all cases.

Small-angle X-ray scattering (SAXS) measurements were performed at the Stanford Synchrotron Radiation Laboratory on Beamline I-4. The white light from the storage ring was vertically focused by using a bent 0.5-m, Pt-coated mirror oriented at 7 mrad with respect to the incident beam. Horizontal focusing was achieved with a bent asymmetrically cut Si(111) crystal oriented to pass X-rays with wavelength of 1.429 Å. Two sets of slits between the crystal and the sample eliminated stray radiation. Detectors before and after the specimen monitored the incident beam flux and the attenuation factor of the specimen. The scattered radiation then passed through an evacuated chamber into a self scanning photodiode array detector with individual pixels with dimensions of $25\ \mu\text{m} \times 1\ \text{mm}$. The scattering profiles were processed via CAMAC electronics and stored on hard disk. The specimens for the SAXS studies on the copolymers were 0.1-mm thick films cast from toluene solutions. The solvent was allowed to evaporate over a period of 24 h, and the films were then placed in a vacuum oven for 5 days at temperatures that increased from ambient to 75°C over this period. Heating the samples in the SAXS experiments was accomplished with a Mettler FP84 hostage that contains a 2-mm hole through which the X-ray beam could pass.⁸ Temperature control was better than $\pm 0.1^\circ\text{C}$.

XPS spectra were recorded with a Kratos XSAM 800 spectrometer using a hemispherical analyzer with a high-resolution band-pass energy of 10 eV. Mg K α radiation with an energy of 1253.6 eV was used, and the operating conditions were 15 KeV and 20 mA. The spectra were recorded at electron takeoff angles normal to the detector. The analysis chamber was at a pressure of 10^{-8} Torr. The copolymer films, ca. $3\ \mu\text{m}$ in thickness, were prepared by casting toluene solutions of the copolymer onto a silicon substrate. The solvent was allowed to evaporate at ambient pressure and temperature. No evidence of beam damage was observed during the XPS experiment. Pure PS and PMMA were separately analyzed to serve as a basis for analysis of the copolymers. Care was taken to ensure that the XPS measurements gave the correct stoichiometric ratio of carbon to oxygen present in PMMA. The details of the XPS analysis of a series of PS/PMMA copolymers may be found elsewhere.⁹

Samples for the ERD measurements were prepared by first casting $3\text{-}\mu\text{m}$ films of the protonated copolymer host onto a silicon wafer. A 200-Å film of either d-PS or d-PMMA was prepared by spin coating toluene solutions of the labeled homopolymers onto a glass substrate. In some cases where the number of segments N_{H} on the deuterated homopolymer chain was comparable to, and larger than, N_{C} , this top layer was made of a blend of very large N_{H} with the lower N_{H} -labeled homopolymer. Here the labeled homopolymer would diffuse rapidly while the large N_{H} species would remain relatively immobile. This would ensure that the volume fraction of the diffusant remained low. This film was transferred onto the previously prepared copolymer host by floating the thin homopolymer film off onto water and then carefully picked up on top of the copolymer-coated silicon wafer. Each sample was then annealed at an elevated temperature for a given period of time under vacuum (10^{-7} Torr) to effect the diffusion process. ERD was then used to determine the volume fraction of deuterated material as a function of depth. The tracer diffusion coefficient, D^* , of the labeled polymer was then extracted from the profile by using a solution to the diffusion equation. A complete description of the ERD experiment and the analysis used can be found elsewhere.¹⁰⁻¹² Concentrations of the diffusant in the copolymer when D^* was evaluated were less than 5% with total diffusion distances on the order of $0.7\ \mu\text{m}$.

Results and Discussion

A. Bulk Morphology. A typical SAXS profile of a solution cast film of SMI is shown in Figure 1 where the intensity is given as a function of the scattering vector q where $q = (4\pi/\lambda) \sin(\epsilon/2)$. Here, λ is the wavelength and ϵ is the scattering angle. The insert at higher scattering vectors is a magnification of the observed scattering by a factor of 20. The data shown have been corrected for both

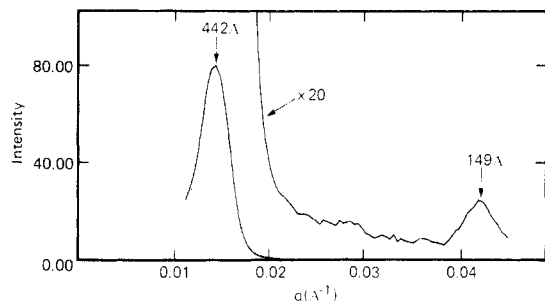


Figure 1. SAXS profile of SMI (PS 42000/PMMA 42000) copolymer at 175 °C. The data as shown have been corrected for parasitic scattering and instrumental noise.

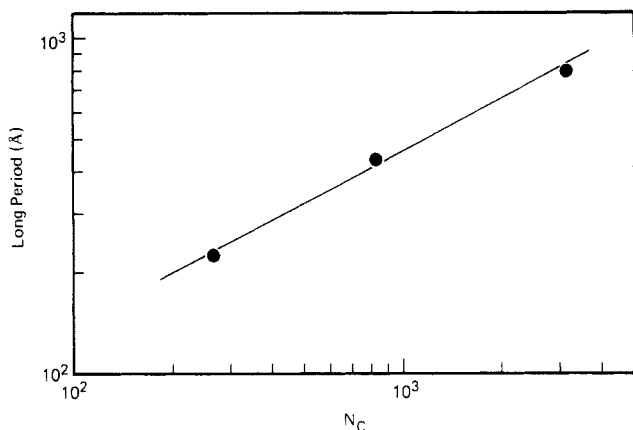


Figure 2. Long period determined from the Bragg spacing corresponding to the position of the peak maxima in the Lorentz corrected SAXS profiles as a function of the number of monomer units in the entire block copolymer. Since the system is symmetric the long period corresponds to twice the domain size.

parasitic and fluctuation scattering. The SAXS from the PS/PMMA copolymers are characterized by an intense first-order reflection and a weak higher order reflection. Observation of the higher order reflection unequivocally proves that these diblock copolymers are microphase separated in contrast to results of a previous study.¹³ The ratio of the Bragg spacing corresponding to the peak position is 2.96 which clearly defines the higher order reflection as a third-order. The absence of the second-order and higher order even reflections is due simply to symmetry conditions since the sizes of the PS and PMMA domains are equal. It is important to note, however, that only the first-order reflection is prominent and the intensity at high scattering vectors is markedly damped. This is a strong indication that the interface between the PS and PMMA domains is diffuse rather than sharp. Evaluation of the diffuse phase boundary shows that for SMI where the long period, i.e., the center to center distance between like phases, is 442 Å, the width of the interface is on the order of 50 Å.

The relatively large width of the diffuse phase boundary would indicate that the Flory-Huggins interaction parameter between the two polymers may be small. This is further supported by the results shown in Figure 2 where the long period or twice the domain thickness is shown as a function of the molecular weight of the copolymer. A power law behavior is seen with an exponent of 0.5. This is consistent with the predictions of theoretical treatment of Liebler¹⁴ for diblock copolymers in the weak segregation limit, i.e., for microphase separated copolymers where the composition or order parameter varies smoothly from one domain to another. Hence, the domain size varies as the radius of gyration of the chains. This may be contrasted

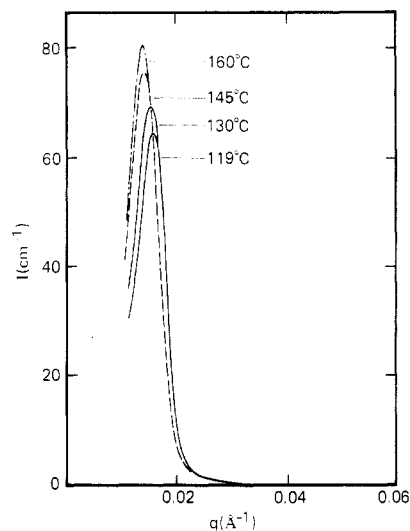


Figure 3. SAXS intensity of SMII as a function of the temperatures indicated. Note the shift in the scattering maximum to smaller scattering vectors and a sharpening and intensification of the reflection with increasing temperature. The data are shown in absolute units.

with systems in the strong segregation limit where the order parameter changes abruptly at the interface.¹⁵ A power law exponent of 0.67 would be expected. It is important to mention that although the copolymers behave as if they are in the weak segregation limit, heating to temperatures in excess of 220 °C did not induce a disordering or phase mixing.¹⁶

Since the diffusion measurements are performed at elevated temperatures, the temperature dependence of the SAXS was investigated. Typical results for the SMI copolymer are shown in Figure 3. Upon heating to temperatures in excess of the glass transition temperatures of each phase the SAXS profiles are seen to intensify, shift to slightly lower scattering vectors, and sharpen. This behavior can be explained by a purification of the phases and a variation in the electron densities and phase volumes by thermal expansion. It is clear, however, that the microphase separated morphology persists at elevated temperatures. Similar results were observed for the SMII and SMIII copolymers. A complete description of the SAXS measurements on the copolymers and their mixtures with the corresponding homopolymers will be reported in a separate paper.¹⁶

One final point that requires mentioning is that the morphology of the diblock copolymers for films 0.1 mm in thickness is isotropically arranged in space. Photographic measurements with the incident beam normal and parallel to the film surface clearly show a circular pattern with a uniform intensity distribution indicating that the lamellar morphology does not preferentially align parallel to the surface over a distance scale that is comparable to the film thickness. Thus, the bulk of the film is comprised of domains of ordered lamellar structures that are randomly arranged in the film.

B. Surface Characterization. While SAXS measurements yield information regarding the details of the bulk of the sample, it does not provide information about the relative surface composition which dictates the fraction of the surface through which the homopolymer chains can freely diffuse. XPS was used to accomplish this. Information regarding the relative composition of both components in the first 50 Å below the surface was obtained by using this technique.

Shown in Figure 4 are a series of XPS spectra for PS, PMMA, and the copolymer SMI. The sole purpose of

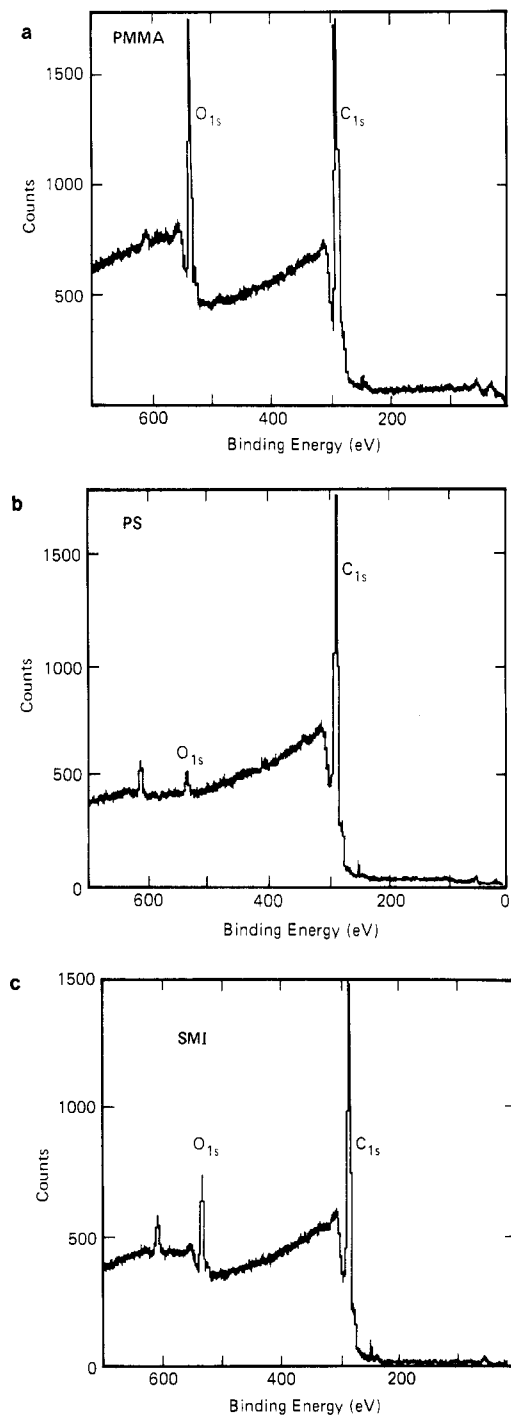


Figure 4. (a) XPS spectrum of PMMA shown as counts versus binding energy. The peaks are assigned to the oxygen 1s and carbon 1s electrons. (b) XPS spectrum of PS. The prominent peak is due to the carbon 1s whereas the minor peak is associated with the oxygen 1s of water and the other (not labeled) in an artifact. (c) XPS spectrum of SMI PS/PMMA copolymer. As before, the major peaks have been assigned whereas the unassigned peaks are artifactual.

these spectra is to show evidence of both PS and PMMA on the surface of the copolymers. A separate paper has been written⁹ concerning an extensive analysis of a number of symmetric diblock copolymer surfaces. Figure 4a shows the whole XPS spectrum of PMMA. At binding energies of 286 and 534 eV are the carbon and oxygen peaks which arise from the ionization of the C 1s and O 1s levels, respectively. High-resolution spectra, not shown here, indicate that there are two oxygen peaks at binding energies of 533.8 and 545.4 eV which are associated with the C=O and C—O—C bonds, respectively. In the vicinity of 290

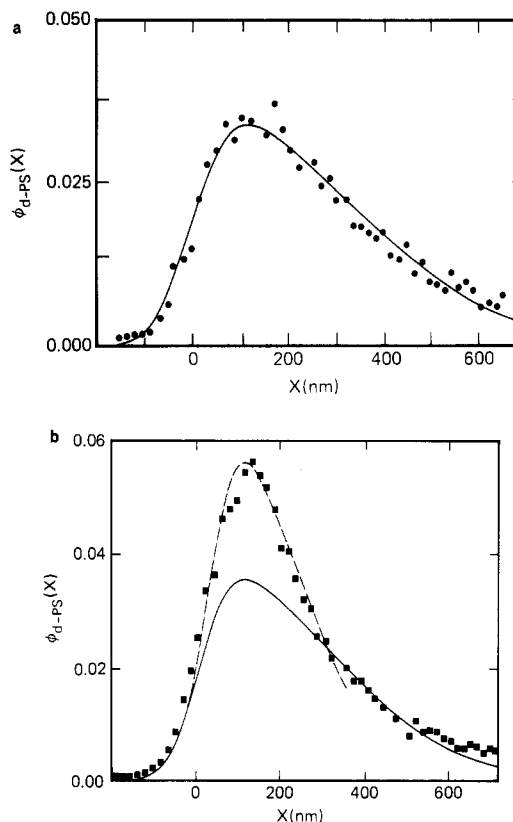


Figure 5. (a) Concentration profile, shown as the volume fraction of d-PS, $\phi_{d-PS}(x)$, as a function of depth x , is for the diffusion of 27 000 d-PS into SMI at 162 °C after 21 min. A tracer diffusion coefficient of $3.8 \times 10^{-13} \text{ cm}^2/\text{s}$ was found here. (b) Volume fraction of d-PS as a function of depth. The data are for the diffusion of 110 000 d-PS into SMI at 163 °C after 290 min. The solid line represents the calculated concentration profile used to obtain a value of D^* of $2.4 \times 10^{-4} \text{ cm}^2/\text{s}$. The slower moving front shown by the calculated dashed line yields $D^* = 9.1 \times 10^{-15} \text{ cm}^2/\text{s}$.

eV are three carbon peaks associated with the C—H, C—O, and O—C=O bonding environments at binding energies 286.4, 288.1, and 290.3 eV, respectively. The XPS spectrum of PS is shown in Figure 4b. At a binding energy of 286.4 eV is the carbon peak. A high-resolution spectrum shows the characteristic shake up transition at 292.8 eV. There is a small peak just below the energy at which the oxygen peaks appear in PMMA shown in this spectrum. This may be a result of adsorbed oxygen on the surface. Finally, in Figure 4c an XPS spectrum of the SMI copolymer cast from solution is shown. Clearly, the oxygen 1s peaks is appreciable. For the SMI, SMII, and SMIII copolymers volume fractions of PMMA at the surface were found to be 0.37, 0.26, and 0.21, respectively. The details of the XPS analysis are published in a separate paper.⁹ Clearly, there are appreciable amounts of both components on the surface of these copolymers. As expected, PS preferentially covers the surface of the copolymers since it has a slightly lower surface free energy. The surface energy of PS is 40.7 dyn/cm and that of PMMA is 41.1 dyn/cm at 20 °C.¹⁷

C. Diffusion Results. Shown in Figure 5a is an ERD profile of volume fraction versus depth of d-PS of weight average molecular weight $M_w = 27\,000$ which was allowed to diffuse into the SMI host for 21 min at 162 °C. The D^* computed from this profile is $3.8 \times 10^{-13} \text{ cm}^2/\text{s}$. This profile is typical of the ones found when the degree of polymerization of the homopolymer N_H is on the order of one-half or less than N_C , the total degree of polymerization of the copolymer for volume fractions of the diffusant less than 5%. For chains of $N_H < N_C/2$ the diffusion coefficient

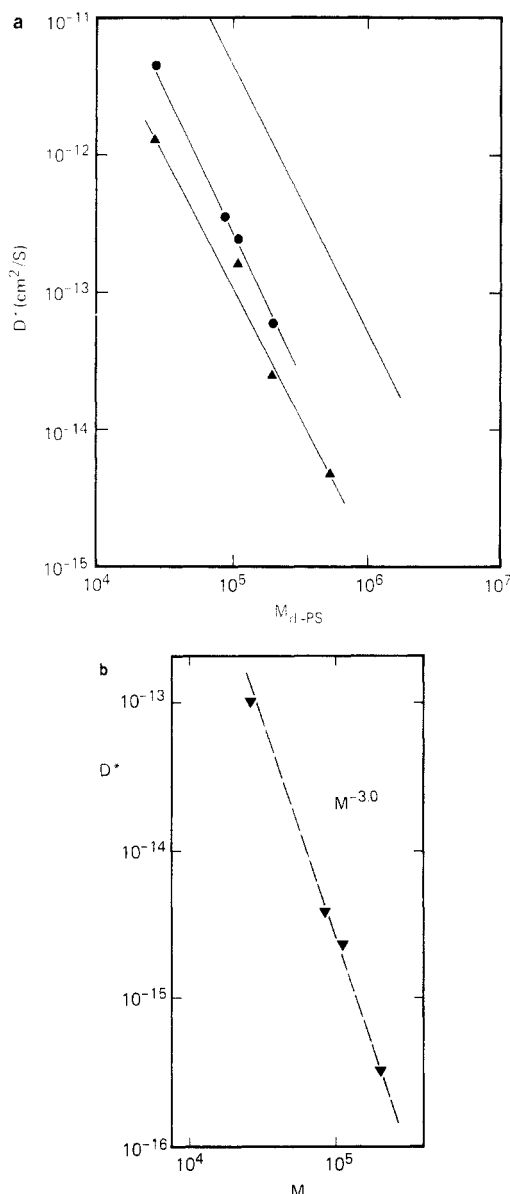


Figure 6. (a) Tracer diffusion coefficient of d-PS as a function of the molecular weight of the tracer d-PS. The diffusion of the tracer into SMII (●), SMIII (▲), and homopolystyrene (solid line) are shown. The diffusion results were obtained at 190 °C. (b) Tracer diffusion coefficient of d-PS into SMI at 162 °C. Strong deviations from the M^{-2} reptation law are observed. Here, the homopolymer molecular weight is greater than the PS block length in the copolymer, and an M^{-3} power law is observed. It is not clear why such a power law should be observed. The line is drawn for illustrative purposes only.

cients extracted from profiles of volume fractions less than 6% of the homopolymer are independent of composition. In the range where the volume fraction of the homopolymer is between 10 and 15% one finds that the diffusion coefficient has dropped by a factor of 2. The diffusion coefficients extracted in the composition regime where the volume fraction of homopolymer that is less than 6% are, therefore, equivalent to tracer diffusion coefficients. Since the solubility of the homopolymer in the block copolymer drops rapidly with its length, it is not surprising that when N_H is comparable to or larger than N_C , the profiles assume a bimodal shape such as the one shown in Figure 5b for volume fractions in the range of 5%. Here it is shown that one portion of the homopolymer diffused rapidly and the other remains relatively immobile in comparison. For the same thickness of the homopolymer film initially at the interface less of the homopolymer diffuses into the co-

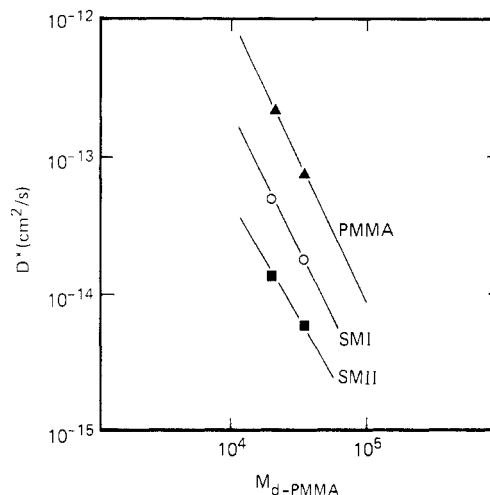


Figure 7. Tracer diffusion coefficient of d-PMMA into SMII (○), SMII (■), and homopoly(methyl methacrylate) (▲) as a function of the molecular weight of d-PMMA. The data were collected at 185 °C.

polymer as N_H increases. Under these circumstances the diffusion coefficient is extracted from the broader of the two distributions which corresponds to the more rapidly diffusing portion.

Plots of the D^* versus N_H of the d-PS into SMII, SMIII, and PS are shown in Figure 6a. These data represent situations in which $N_H < N_C$. We were able to ensure that in this regime the diffusion coefficients extracted were within the tracer limit. Each set of data may be described by

$$D^*_{d-PS} = KM^{-\alpha} \quad (1)$$

where the value of α is 2.1, 1.9, and 2.0 for diffusion into SMII, SMIII, and PS, respectively. Hence, within experimental error, each set of data exhibits the same power law dependence. It is also clear from this figure that d-PS chains diffuse into the copolymer hosts at rates about an order of magnitude lower than into the PS host. Figure 6b shows data representing the diffusion of d-PS into SMI. In this case the homopolymer chain lengths are much higher than N_C . The diffusion coefficients determined here are not equivalent to tracer diffusion coefficients and are concentration dependent. This set of data exhibits a stronger dependence on N_H than the set in Figure 6a. The line drawn through the data shows a limiting power law dependence of -3 . We expect the slope to become steeper with increasing N_H . The limited set of data in Figure 7 which shows the diffusion of d-PMMA into pure PMMA and into the copolymers shows qualitatively the same trend as that shown in Figure 6.

We believe that during the diffusion process the homopolymer chains are restricted primarily to their corresponding domains for a number of reasons. SAXS measurements of mixtures of the copolymer with homopolymers show that the homopolymer chains are restricted to their respective domains at concentrations of homopolymer which are somewhat larger than the ones currently considered in this study even in cases where N_H is somewhat larger than N_C .^{16,20} Further experiments suggest that the diffusion of d-PS (d-PMMA) into high molecular weight PMMA (PS) occurs at rates that are considerably lower than into the copolymer hosts.¹⁸ In addition further evidence is provided by the strong dependence of D^* on N_H in Figure 6 where it is observed that the diffusion coefficient decreases more rapidly than N_H^{-2} when $N_H \gtrsim N_C$. This is expected since in a phase-separated copolymer structure the solubility of the homopolymer in the co-

polymer drops rapidly with increasing N_H .¹⁹ The diffusion process becomes highly concentration dependent. Furthermore, the sample processing conditions, which will be addressed later, have a dramatic effect on D^* which is expected if the copolymers are phase-separated. Finally, temperature-dependent measurements, which will be published in a separate paper,²⁰ are consistent with the view that homopolymer chains are restricted primarily to their respective domains during the diffusion process.

A number of points may be inferred from the results in Figures 6 and 7. It is clear that PS and PMMA form continuous phases since the length scales probed in this experiment are on the order of $0.7 \mu\text{m}$ and the domain dimensions are on the order of a few hundred angstroms. The results also suggest that the PS and PMMA domain sizes are of the same order since the diffusion rates of both homopolymers into their respective homopolymer hosts occur more slowly into the copolymer hosts by the same factor. This is consistent with the SAXS findings mentioned earlier. The observation of the reptation scaling exponent suggests that the chains diffuse in essentially the same environment; i.e., no major structural changes occur in the bulk during the diffusion process. This, however, does not preclude structural rearrangements that occur initially at the interface which are necessary so as to allow the homopolymer chains to penetrate into the bulk.

Figures 6 and 7 also show that the homopolymers diffuse into the copolymer hosts about an order of magnitude lower than into their respective homopolymer hosts. We believe that this is primarily related to the tortuosity, the spatial orientation of the domains, and a partitioning effect. The possibility of interfacial resistance is ruled out since the XPS results indicate that there are appreciable amounts of both components on the copolymer surface. In addition the presence of interfacial resistance would be inconsistent with the observed -2 power law dependence of D^* on N_H . With regard to the diffusion of homopolymers into homopolymers a number of factors influence D^* which may influence the diffusion of homopolymer chains into the copolymer hosts. These factors are the monomeric friction coefficient, ζ , and the number of monomer segments between entanglement, N_e . For the diffusion of homopolymers into homopolymers the tracer diffusion coefficient is given by²¹

$$D^*_{HH} = (4/15)[N_e k_B T / \zeta] N^{-2} \quad (2)$$

where k_B is the Boltzmann constant and T is the absolute temperature. The conformation of chains in the domains may affect N_e , but in the present situation this effect should be negligible since SAXS measurements indicate that the domain size scale as the radius of gyration suggesting that the conformation of chains in the domains is not very different from that present in a pure homopolymer. On purely physical grounds the monomeric friction coefficient is not expected to be appreciably influenced by the molecular configuration. The average domain size should affect ζ . However, for the cases studied here the effects should be unimportant since the domains are larger than the radius of gyration of each diffusing chain. The SAXS measurements show that the PS and PMMA phases are relatively pure. It follows that any phase mixing is small and would, therefore, have little effect on D^* . In addition, we have conducted a series of experiments¹⁹ which show that the diffusion of d-PS into PS and into the copolymers have the same temperature dependence. The same observation was made for the diffusion of d-PMMA. Since the friction coefficient controls the temperature dependence of D^*/T , one may assume, on the basis of the temperature-dependent studies

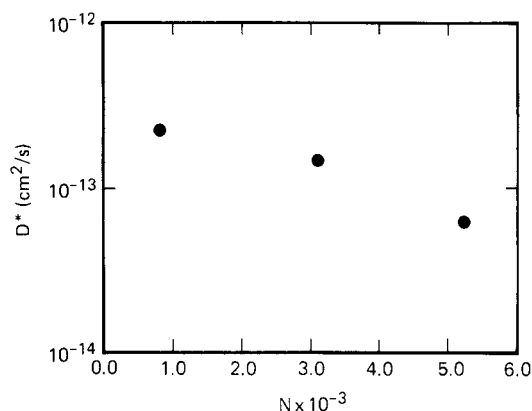


Figure 8. Tracer diffusion coefficient of d-PS ($M_w = 27\,000$) into SMI, SMII, and SMIII copolymers where N is the total number of monomer segments in the copolymer.

and the preceding arguments, that the monomeric friction coefficient is not responsible for the difference in diffusion rates. The SAXS measurements suggest that the copolymer structure is characterized by short-range order and the diffusion measurements indicate that the phases are continuous. Consequently, it is reasonable to conclude that the comparatively low diffusion rates measured are due to three major factors. They are the spatial orientation of the domains, a partitioning effect which results because only half of the volume of the bulk sample is accessible to the homopolymer chains, and the tortuosity of the domains.

For discussion purposes, assume that the diffusion coefficient of the homopolymers into copolymer, D_{HC} is related to D_{HH} by

$$D_{HC} = kftD_{HH} \quad (3)$$

k is related to the average orientation of the domains defined by $\langle \sin \phi \rangle$ where ϕ is the angle between the surface normal and a vector normal to the interface between phases. If order persisted on a large scale and the lamellae were parallel to the surface, then $k = 0$. Realistically, however, this would simply mean that the diffusion rate would be considerably lower. If all the domains were normal to the surface, then $k = 1$ and f is the volume fraction of the bulk that is available for diffusion; in this case it is $1/2$. The final factor t is related to the tortuosity, i.e., the continuity of the individual phases. In general the more irregular microstructure, the more tortuous the path is in which the homopolymer diffuses and the smaller is the value of t . For obvious reasons neither k nor t may be accurately calculated in this system, and, in fact, may not be independent variables. They are separated here for emphasis only.

On unusual feature of the tracer diffusion coefficient of the homopolymer chains into the copolymer host is that it decreases as the molecular weights of the blocks increase. This is exemplified by the data for the diffusion of d-PS ($M_w = 27\,000$) into SMI, SMII, and SMIII shown in Figure 8. This is unexpected since the SAXS results clearly show that the long period and, consequently, the domain spacing increases with increasing molecular weight. This cannot be attributed to a surface coverage effect since the surface coverage of PS exhibits an opposite trend. These results are evidently a reflection of the morphology. The higher molecular weight copolymers form more irregular structures than the lower molecular weight analogues when the solvent evaporation rates are the same during the sample preparation process. The viscosity of the solutions increases rapidly with increasing N_H . In solution the chains attempt to rearrange themselves in a configuration that

would minimize the total free energy of the system. It is much more difficult for highly viscous systems to undergo a cooperative diffusion process that is necessary to accommodate the formation of this equilibrium morphology. Since the solvent evaporation rates in the three systems are the same, the lower molecular weight systems, which are less viscous, would have progressed to a more regular structure than the others during this time. Such observations have been made previously with polystyrene-polyisoprene copolymers.²² It should be reiterated, however, that the solvent extraction rates are too rapid to allow the formation of an equilibrium morphology in any of the systems. The results discussed below confirm this.

It is well-known that the conditions under which a block copolymer is prepared has a pronounced effect on the microstructure. The rate of solvent evaporation and thermal treatment can markedly alter the phase purity, the order of the domain structure, and the nature of the microphase separation. For example, the SAXS data shown in Figure 3 clearly show such effects. Structural changes would be expected to change the transport of the homopolymer through the block copolymer. To address this point, the tracer diffusion coefficient of d-PS into SMII and d-PMMA into SMI were measured where the copolymer films were annealed for different periods of time at 174 °C and where the casting solvent was varied. The results of these studies are shown in parts a and b of Figure 9. The data are shown as the ratio of the measured tracer diffusion coefficient to that measured in the homopolymer case. The effect of casting solvent is clearly seen by the differences observed when toluene or methylene chloride is used. The latter solvent evaporates more rapidly and, thus, gives rise to a more disordered microstructure. Since methylene chloride does not selectively solvate PS or PMMA preferentially, then a totally different microstructure would not be expected. Consistent with this, the tracer diffusion coefficients of d-PS and d-PMMA into the copolymer films cast from methylene chloride were both found to be about a factor of 2 lower than those prepared from toluene. Heating the copolymer films cast from toluene to 174 °C for 3 h brings about a further increase in the tracer diffusion coefficient. Similar results are found if the copolymer films are exposed to a toluene environment for two hours. These data suggest that the microphase separation becomes more ordered with these treatments. Finally, upon annealing the copolymer films for extended periods of time at 174 °C, i.e., for 24 h, the tracer diffusion coefficient drops by at least a factor of 3 in both cases. A similar result is found if the films are exposed to solvent for an extended period of time, i.e., 24 h. Since the microphase separation is improved with either of these treatments, then it can only be concluded that for reasonably short annealing times the long-range order increases and at longer times the microphases reorient and adopt an orientation that is more parallel to the film surface. Given that there is a difference in the surface energies of the two components, such a reorientation would not be unusual, and recent studies on polystyrene-polybutadiene copolymers by Henkee and Thomas²³ support this observation. The reorganization process in the PS/PMMA system is much slower. For this reason it is an ideal system for studies of the effects of microdomain orientation, tortuosity, and partitioning on the diffusion of homopolymers into block copolymers.

Conclusion

The results presented here represent only a preliminary study of the diffusion of homopolymers in copolymer systems. It was found that deuteriated polystyrene chains

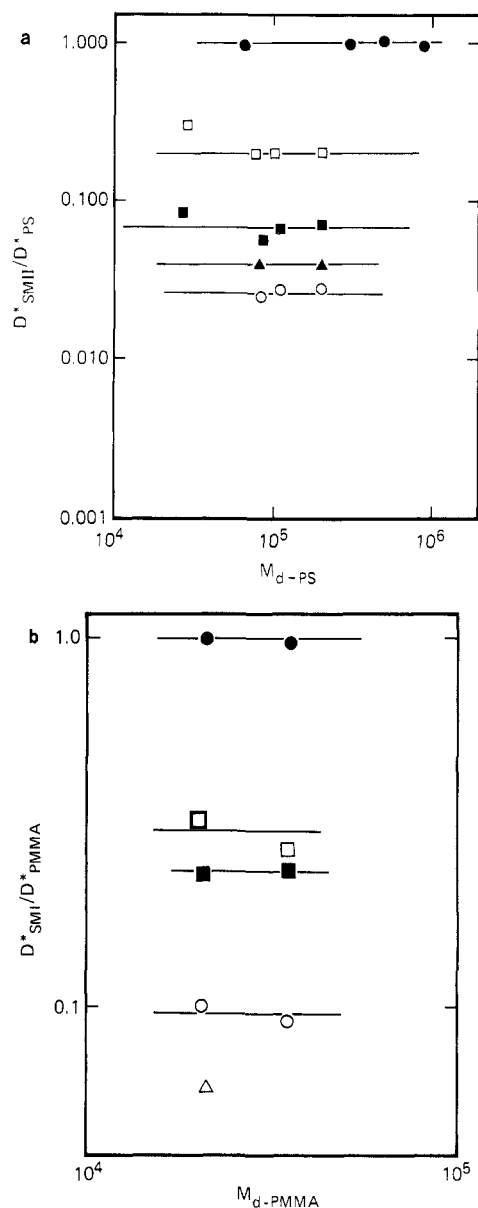


Figure 9. (a) Ratio of the log of the tracer diffusion coefficient of d-PS into SMII to that in homopolystyrene. The results of the homopolystyrene (●) are shown for reference. The data represent results taken for SMII films cast from methylene chloride (▲) and toluene (■) and from toluene cast films annealed at 174 °C for 3 h (○) and at 174 °C for 24 h (□). All diffusion data were taken at 154 °C. (b) Ratio of the d-PMMA tracer diffusion coefficient in SMI to that in homopoly(methyl methacrylate). The homopolymer results are shown for reference. These data are for copolymer films cast from methylene chloride (○) and toluene (■) and toluene cast films annealed at 174 °C for 3 h (□) and 24 h (△). All diffusion data shown were obtained at 162 °C.

diffuse into the diblock copolymer structures at a rate inversely proportional to the square of their length. The diffusion of d-PMMA chains into the copolymers is qualitatively similar. This scaling behavior was observed independent of the sample processing conditions. The tracer diffusion coefficients are just over an order of magnitude smaller for diffusion into the copolymers than that measured for the diffusion into their respective homopolymer hosts. This large difference, we believe, is primarily related to the tortuosity and orientation of the microphase separated domains and not due to interfacial effects. Hence, the diffusion of homopolymers into copolymer systems is controlled by geometrical factors in addition to the molecular weight between entanglement

and the monomeric friction coefficient which control the diffusion of homopolymers into homopolymer diffusion. It has also been shown that the rate of solvent evaporation and annealing treatments of the host copolymer markedly influence the structure as seen by changes in the transport properties. Finally, reorganization processes may occur at the homopolymer-copolymer interface or in the bulk. However, the time scales for this are very much different than that of the diffusion process.

Acknowledgment. We thank H. Ito of the IBM Almaden Research Center for providing the deuterated PMMA. We thank Dr. T. Christensen for the XPS measurements on the copolymer specimens. R.J. is grateful to the IBM World Trade Organization and to the IBM Almaden Research Center for the possibility of visiting the latter facility. M.G. and R.J. are very much indebted to "Services de la Programmation de la Politique Scientifique" (Brussels) for financial support. M.G. thanks the Fonds National de la Recherche Scientifique for a fellowship. Part of this work was performed at the Sandia National Laboratories and was supported by the U.S. Department of Energy under Contract DE-AC04-76DP00789.

Registry No. (S)(MMA) (copolymer), 106911-77-7.

References and Notes

- (1) For a recent review see: Tirrell, M. V. *Rubber Chem. Tech.* **1984**, *57*, 523.
- (2) Doi, M.; Edwards, S. F. *J. Chem. Soc., Faraday Trans. 2* **1978**, *1809*, 1818.
- (3) deGennes, P. G. *J. Chem. Phys.* **1971**, *55*, 572.
- (4) Graessley, W. W. *J. Polym. Sci., Polym. Phys. Ed.* **1980**, *18*, 27.
- (5) Hasegawa, H.; Hashimoto, T. *Macromolecules* **1985**, *18*, 589.
- (6) Ouhadi, T.; Fayat, R.; Jérôme, R.; Teyssie, Ph. *Polym. Commun.* **1986**, *27*, 212; U.S. Patent 4 461 874, 1984.
- (7) Ito, H.; Russell, T. P.; Wignall, G. D. *Macromolecules*, in press.
- (8) Russell, T. P.; Koberstein, J. T. *J. Polym. Sci., Polym. Phys. Ed.* **1985**, *23*, 1109.
- (9) Green, P. F.; Christensen, T. M.; Russell, T. P. *Macromolecules*, in press.
- (10) Mills, P. J.; Green, P. F.; Palstrom, C. J.; Mayer, J. W.; Kramer, E. J. *Appl. Phys. Lett.* **1984**, *45*, 958.
- (11) Green, P. F.; Mills, P. J.; Kramer, E. J. *Polymer* **1986**, *27*, 1063.
- (12) Green, P. F.; Doyle, B. L. *Nucl. Instrum. Meth. Phys. Res., Sect. B* **1986**, *B18*, 64.
- (13) Benoit, H.; Wu, W.; Benmouna, M.; Mozer, B.; Bauer, B.; Lapp, A. *Macromolecules* **1985**, *18*, 986.
- (14) Leibler, L. *Macromolecules* **1980**, *13*, 1602.
- (15) Ohta, T.; Kawasaki, K. *Macromolecules* **1986**, *19*, 2621.
- (16) Russell, T. P.; Jérôme, R., in preparation.
- (17) Wu, S. *Polymer Interfaces and Adhesion*; Marcel Dekker: New York, 1982.
- (18) In cases where one tries to diffuse d-PMMA into PS one obtains what appears to be a diffusion profile. This results from the fact that the PMMA forms very small spherical particles on the surface of PS, and since PS is viscous, these spherical particles become incorporated into the PS matrix. This occurs over a certain molecular weight regime, and the behavior is not consistent from one temperature to another.
- (19) Whitmore, M. D.; Noolandi, J. *Macromolecules* **1985**, *18*, 2486.
- (20) Green, P. F.; Russell, T. P.; Jérôme, R.; Granville, M. *Macromolecules*, in press.
- (21) Graessley, W. W. *Faraday Symp. Chem. Soc.* **1983**, No. 18, 1.
- (22) Hashimoto, T.; Nagatoshi, K.; Todo, A.; Hasegawa, H.; Kawai, H. *Macromolecules* **1974**, *7*, 364.
- (23) Henke, C. S.; Thomas, E. L.; Fetters, L. J. *J. Mater. Sci.*, in press.

Predictions of the Ability of Solution Dynamics Experiments to Characterize Long-Chain Structure in Flexible Homopolymers

Robert L. Sammler[†] and John L. Schrag*

Department of Chemistry and Rheology Research Center, University of Wisconsin, Madison, Wisconsin 53706. Received December 17, 1987; Revised Manuscript Received April 8, 1988

ABSTRACT: Extensive predictions are presented to illustrate the ability of linear viscoelasticity and oscillatory flow birefringence experiments to characterize long-chain structure in flexible homopolymers. The predicted dilute-solution, low-shear-rate dynamic properties are based on a recent generalization of the bead-spring model that enables such properties to be computed efficiently for any chain of identical beads connected by Hookean springs. Highly symmetric chains with linear, star, H, comb, ring, or cyclic-comb geometry are emphasized. Ways to identify samples with these geometries from their solution properties are presented, as well as ways to characterize the sizes of the branches and backbone, the number of branches, and location of branches attached to the backbone. Characterization is expected to be difficult only for small chains and for the determination of the number of branches in star or starlike chains when it exceeds about 8.

I. Introduction

Long-chain branches attached to straight-chain or cyclic backbones are common and distinctive structural features of macromolecules and yet their characterization, in terms of branch and backbone size or the number and location of the branches, remains challenging even for the simplest highly symmetric chains. The potential of solution dynamics measurements for characterization of such structural features was recognized long ago. However, only in the last 15 years have there been sufficient advances in both the measurement and quantitative prediction of solution dynamics to enable a pragmatic evaluation of this

potential. Flow properties such as the complex viscosity coefficient η^* (linear viscoelasticity (VE) experiments¹⁻⁶) and the complex mechanooptic coefficient S^* (linear oscillatory flow birefringence (OFB) experiments³⁻⁸) can now be measured over many decades of shearing frequency with sufficient accuracy to be extrapolated to infinite dilution; such data are required to probe the wide range of time scales associated with conformational motions of macromolecules in solution and to interpret long-chain structure from dynamic properties in which interchain interactions are negligible. Bead-spring models are now formulated^{9,10} to enable predictions of such properties to be efficiently and accurately computed for an idealized flexible homopolymer chain of any geometry, for chains of finite size, and for any degree of hydrodynamic interaction; these computations are needed for the assessment of long-chain

[†] Current address: Polymer Products Department, Experimental Station, E. I. du Pont de Nemours and Co., Inc., Wilmington, DE 19898.